Textural and Structural Properties of Zirconium Dioxide Depending on Synthesis Methods and Precursor Type

Mariy Savastyanova

mariysav75@gmail.com

Institute of Technical Chemistry of UB RAS– affiliation of the Perm Federal Research Centre of the Ural Branch of the Russian Academy of Sciences

Natalya Kondrashova

Institute of Technical Chemistry of UB RAS– affiliation of the Perm Federal Research Centre of the Ural Branch of the Russian Academy of Sciences

Konstantin Ukhin

Institute of Technical Chemistry of UB RAS– affiliation of the Perm Federal Research Centre of the Ural Branch of the Russian Academy of Sciences

Viktor Valtsifer

Institute of Technical Chemistry of UB RAS– affiliation of the Perm Federal Research Centre of the Ural Branch of the Russian Academy of Sciences

Research Article

Keywords: zirconium dioxide, template hydrothermal synthesis, ultrasonic treatment, monoclinic and tetragonal modifications, specific surface area, sorption isotherms, particle shape

Posted Date: June 9th, 2025

DOI: https://doi.org/10.21203/rs.3.rs-6816571/v1

Additional Declarations: No competing interests reported.

Version of Record: A version of this preprint was published at Journal of Sol-Gel Science and Technology on August 14th, 2025. See the published version at https://doi.org/10.1007/s10971-025-06892-5.

TEXTURAL AND STRUCTURAL PROPERTIES OF ZIRCONIUM DIOXIDE DEPENDING ON SYNTHESIS METHODS AND PRECURSOR TYPE

M.A. Savastyanova*, N.B. Kondrashova, K.O. Ukhin, V.A. Valtsifer

Institute of Technical Chemistry of UB RAS– affiliation of the Perm Federal Research Centre of the Ural Branch of the Russian Academy of Sciences, Academician Koroleva st., 3, Perm, Russia 614013

Corresponding author *e-mail: mariysav75@gmail.com

Graphical abstract

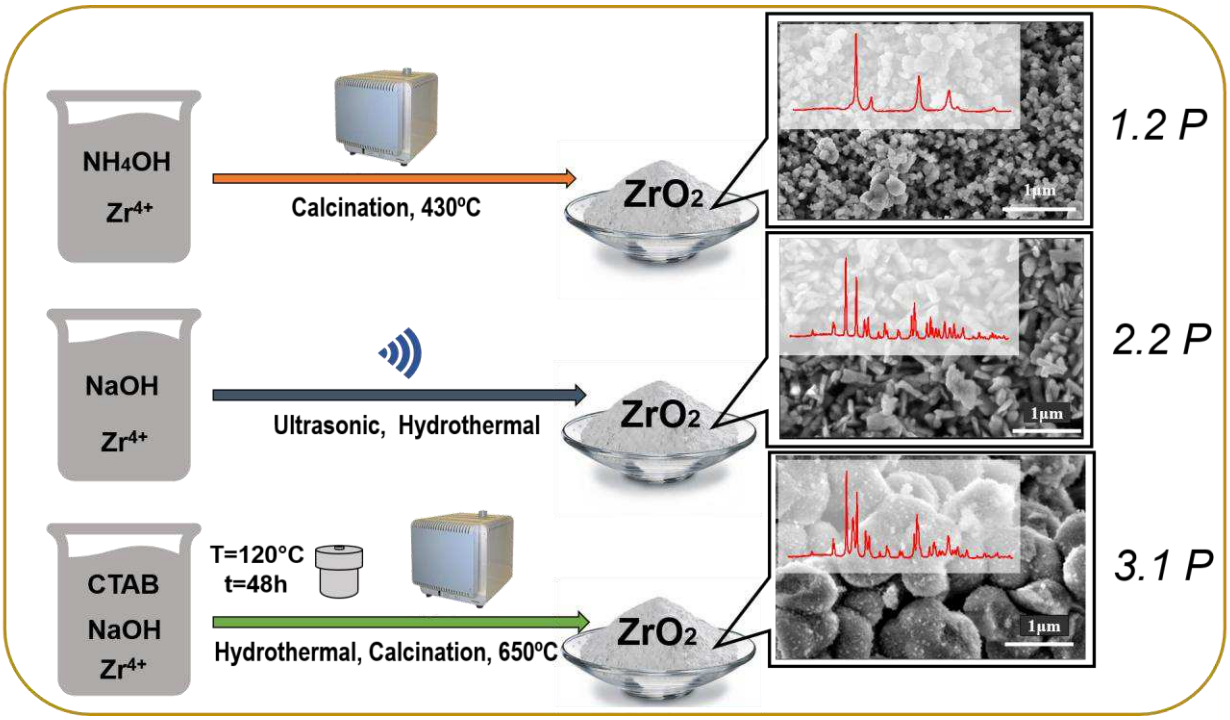

Highlights:

- Methods of producing zirconium dioxide with a small crystallite size ranging from 5 to 9 nm, a specific surface area of approximately 150 m^2/g, and a pore volume below 0.25 cm^3/g with a narrow size distribution are proposed.
- It has been established that the phase composition of the ZrO2 samples obtained by different templateless precipitation methods is mainly determined by the method of synthesis.
- The nature of precursors of zirconium dioxide has a strong effect on its textural and structural properties in the case when the ZrO_2 samples are prepared by applying different types of the template hydrothermal synthesis.

Keywords:

zirconium dioxide, template hydrothermal synthesis, ultrasonic treatment, monoclinic and tetragonal modifications, specific surface area, sorption isotherms, particle shape

Abstract

This paper provides a comparative assessment of the influence of the nature of precursors of zirconium dioxide and the methods of its production, including the application of such additional physical and chemical factors as template introduction, ultrasound and hydrothermal ageing, on the textural and structural properties of ZrO_2.

Methods of producing zirconium dioxide with a small crystallite size ranging from 5 to 9 nm, a specific surface area of approximately 150 m^2/g, and a pore volume below 0.25 cm^3/g with a narrow size distribution are

proposed. It has been established that the phase composition of the ZrO_2 samples obtained by different templateless precipitation methods is mainly determined by the method of synthesis. No significant effect of the nature of the ZrO_2 (zirconium oxysalts) precursors on the structural properties of the studied samples was observed.

The textural and structural properties of the ZrO_2 samples, prepared in an aqueous alkaline medium by different template hydrothermal synthesis methods in the presence of cationogenic surfactant - cetyltrimethylammonium bromide (CTAB), show strong dependence on both the nature of the ZrO_2 precursors and the ratio of the main components.

It is shown that, when ultrasound and hydrothermal treatment are used for synthesis of ZrO_2, a sequence of additional physical factors greatly influences the properties of the obtained samples.

1. Introduction

Due to its excellent resistance to high temperatures and corrosion, zirconium dioxide ZrO_2 has been extensively used in industrial applications, in medicine, and in research in the field of creating new materials. Thanks to its thermal and mechanical stability and acid-base properties, zirconium dioxide is an effective catalyst for use in many physical and chemical processes [1-6].

There are two main groups of methods for producing zirconium dioxide: high temperature synthesis techniques that include processing of zircon raw materials (most effective in large-scale applications), and wet chemical methods which are based on transformation of zirconium compounds in aqueous solutions. Almost all types of high temperature synthesis allow production of materials in which zirconium dioxide is in a crystal phase, forming monoclinic m-ZrO_2, tetragonal t-ZrO_2, or cubic c-ZrO_2 modifications or their mixtures [7, 8]. The application of wet chemical methods (precipitation methods, sol-gel technologies) makes it possible to obtain, along with crystalline structures, the amorphous phase of zirconium dioxide [9, 10].

Wet chemical methods for producing zirconium dioxide are often coupled with different physical factors that affect the reaction medium. A combination of physical and chemical methods may be quite promising for synthesis of zirconium dioxide with a narrow particle size distribution and a controlled ratio of crystalline phases [11-16].

The temperature range of existence of polymorphic modifications is known to be strictly limited. Despite the fact that the monoclinic phase of zirconium dioxide is thermodynamically stable (to 1170 ºC), some authors reported that the high temperature modifications of ZrO2 - tetragonal (1170 ºC - 2280 ºC) and cubic (>2280 ºC) - exhibit the highest catalytic activity [3]. Therefore, the high-temperature phases of zirconium dioxide, which is intended for use at temperatures below 1000 ºC, are in need for stabilization. The metal oxides of group IIIB in Mendeleev's Periodic Table of Elements, namely, oxides of yttrium, scandium, lanthanum and lanthanides, are most often used for this purpose [15, 16].

It is also reported that complete stabilization of the high-temperature phases of zirconium dioxide can be attained by applying the ZrO_2 synthesis methods intended to reduce its crystallites and particle sizes [17-21]. Zirconium alkoxides are best suited for using as precursors in preparation of zirconium oxide for catalysis and sorption processes. It is recognized that the hydrolysis of zirconium dioxide leads to the formation of hydroxyalkoxide complexes. During the polycondensation reaction, these complexes can easily polymerize into structures with a large number of repeating units. Amorphous hydrated oxides that contain residual alkoxide groups are produced at the first stage of the reaction, and their subsequent drying and heat treatment promote the formation of crystalline products [13, 22, 23].

Collected data on the hydrolysis of inorganic zirconium salts suggest that the reaction medium contains not only zirconium oxides but also inorganic anions (Cl-, NO_3-, etc.). Therefore, in the case of inorganic zirconium

salts, the intermediate synthesis products must be thoroughly washed. Since the aqueous solutions of zirconium salts are subject to hydrolysis, which causes complex cations of different compositions to appear, the key properties of the oxide material are determined to a great extent by reactions proceeding at this stage. Heat treatment helps to speed up the processes of hydrolysis and subsequent polycondensation of intermediates, which makes it possible to obtain zirconium dioxide particles [11-14].

Although there are a great number of publications related to the production of ZrO_2 and investigation of its properties, the study of its textural properties, such as a specific surface area and porosity, depending on the applied ZrO_2 synthesis method has not received sufficient attention. At the same time, according to the literature, it is the high-temperature modifications of zirconium dioxide with a small particle size that exhibit the best acid-base properties, which is of primary importance in choosing a catalyst base [3]. Therefore, the objective of this paper is to perform a comparative assessment of the specific surface area, porous structure, phase composition and particle morphology of zirconium dioxide samples obtained by different types of the template and template-free synthesis of zirconium particles in which the alkoxides of zirconium and its inorganic oxysalts are used as precursors.

2. Experimental section

Methods for producing zirconium dioxide were chosen by analyzing literature and experimental data.

In this work, zirconium alkoxides – zirconium propylate 70% solution in 1-propanol $Zr(C_3H_7O)_4$, Sigma-Aldrich, Germany, samples *P*, and zirconium butylate 80% solution in 1-butanol $Zr(C_4H_9O)_4$, Sigma-Aldrich, samples *B,* as well as zirconium oxysalts – zirconium oxychloride octahydrate $ZrOCl_2 \cdot 8H_2O$, Sigma-Aldrich, samples *Ch* and zirconyl nitrate dehydrate $ZrO(NO_3)_2 \cdot 2H_2O$, Sigma-Aldrich, samples *N,* are used as the precursors of zirconium oxide.

2.1. Synthesis of zirconium dioxide

The samples of zirconium oxides (hydroxides) were synthesized using different variants of the precipitation method both with and without such additional physical-chemical factors as surfactants, ultrasonic and hydrothermal treatment.

1. Methods of templateless precipitation

1.1. precipitation in an alcohol-ammonia medium by mixing the reaction components in molar ratios 20 H_2O : 10 C_2H_5OH : 2 NH_4OH : 1 Zr^{4+} using a magnetic stirrer during 5 h at a room temperature, followed by removal of a liquid phase, washing and drying of precipitates at 100 ºC – samples *1.1P;1.1B; 1.1Ch, 1.1N*;

1.2. calcination of samples *1.1P,1.1B, 1.1Ch, 1.1N* at a temperature 430 ºC –samples *1.2P; 1.2B; 1.2Ch; 1.2N*.

2. Methods of templateless precipitation coupled with ultrasound treatment and hydrothermal ageing

2.1. ultrasound treatment of a 2% aqueous suspension of the ZrO_2 samples synthesized by method *1.1,* using an ultrasonic homogenizer Bandelin SONOPULS (Germany) for 30 min (oscillation frequency 20 kHz), followed by hydrothermal ageing of these samples at 250 ºC during 24 h, filtration, washing, and drying of a precipitate at 100 ºC – samples *2.1P; 2.1B; 2.1Ch; 2.1N*;

2.2. 30 min ultrasonic treatment during the precipitation of zirconium hydroxides when mixing the reaction components in molar ratios 315 H_2O : 4 C_3H_7OH: 14 NaOH : 1 Zr^{4+}, followed by hydrothermal ageing of the reaction mixture at 250 ºC during 24 h, filtration, washing, and drying of a precipitate at 100 ºC – samples *2.1P; 2.1B; 2.1Ch; 2.1N*; *2.2P, 2.2B, 2.2Ch, 2.2N*.

3. Methods of template hydrothermal synthesis in the presence of a cationogenic surfactant - cetyltrimethylammonium bromide (CTAB), followed by the hydrothermal ageing of a reaction mixture

3.1. Methods of template hydrothermal synthesis under conditions of hydrothermal ageing at 120ºC during 48 h, filtration of a precipitate, its washing to the pH value of the medium, drying and thermolysis of the organic component at a temperature 650 ºC during 3 h; the mole ratios of the reaction components: 100 H_2O : 0,44 CTAB : 0,4 NaOH : 1 Zr^{4+} – samples *3.1P; 3.1B; 3.1Ch; 3.1N*;

3.2. Methods of template hydrothermal synthesis with a large amount of a precipitant under conditions of hydrothermal ageing at 120 ºC during 48 h, filtration of a precipitate, its washing to the pH value of the medium, drying and thermolysis of the organic component at a temperature 650 ºC during 3 h; the mole ratios of the reaction components: 100 H_2O : 0,44 CTAB : 2 NaOH : 1 Zr^{4+} – samples *3.2P; 3.2B*; *3.2Ch; 3.2N*;

3.3. Method of template hydrothermal synthesis in large volumes of aqueous ammonia solutions in the presence of a cationogenic surfactant - cetyltrimethylammonium bromide (CTAB), followed by the hydrothermal ageing at 100 ºC during 12 h, , filtration of a precipitate, its washing to the pH value of the medium, drying and thermolysis of the organic component at a temperature 650 ºC during 3 h; the mole ratios of the reaction components: 6000 H_2O : 0,22 CTAB : 240 NH_4OH : 1 Zr^{4+} – samples *3.3P; 3.3B; 3.3Ch; 3.3 N*.

2.2 Methods

The properties of synthesized zirconium dioxide samples were investigated by different physical-chemical methods of analysis.

The TGA/DSC 1 thermal analyzer (METTLER-TOLEDO, Switzerland) was used to determine the temperatures of decomposition of zirconium dioxide precursors and intermediate synthesis products and the phase transition temperature in an air atmosphere at a heating rate of 10ºC/min in the temperature range 25–1000 ºC.

After degassing the test material in vacuum at 100 ºC during 3 h, the textural properties of the zirconium dioxide samples obtained in different ways were investigated by the low-temperature nitrogen sorption method using the ASAP 2020 device (Micromeritics, the USA). The specific surface area of the samples ((S_{BET}) was determined by the BET method, and the pore volume and the pore size distribution were obtained from the desorption isotherms by applying the BJH method.

The phase composition of the synthesized zirconium dioxide samples was determined by the X-ray phase analysis (XRD) on an XRD-7000 (Shimadzu, Japan) with CuK_α-radiation (λ_{cp} = 1,54184 Å) in the angular range 10–80º with a step 0,01–0,005º. The XRD patterns of all samples were decoded using the JCPDS card. The average crystallite size was determined by the Scherrer method: $D_{PФA} = K\lambda/(\beta cos\Theta)$, where K = 0,89; λ = 1,54056 Å; β is the half-width of the reflection (100), rad.; Θ is the diffraction angle of reflection. The mass ratio of the crystalline phases in the samples was determined by the Rietveld method using the Siroquant software v4.

The IR spectra were recorded in the region 400-4000 cm^{-1} using a Vertex80V IR Fourier spectrometer (Bruker, Germany).

The average particle size ($D_{CЭM}$) and the particle shape of the obtained ZrO_2 samples were examined by scanning electron microscopy (SEM) using a FEI Quanta FEG 650 (Thermo Fisher Scientific, Netherlands) on a secondary electron detector at the accelerating voltage of 10 kV.

3. Results and discussion

3.1 The structural properties of zirconium dioxide produced through various methods of template-less precipitation synthesis

Table 1 and Figs.1-5 provide information about the structural properties of the zirconium dioxide samples synthesized following different methods and using different precursors.

According to the results of XRD (Table 1), the expected precipitation products of zirconium alkoxides and salts in an aqueous-alcoholic medium by ammonia solutions are the X-ray amorphous hydrated zirconium oxides (*samples 1.1P,1.1B, 1.1Ch, 1.1N*).

Based on the thermal analysis data and the results of literature search, we suggest that the crystallization of amorphous precipitation products proceeds at 430 ºC either with zirconium alkoxides as precursors to ZrO_2 or its oxysalts.

After the calcination of amorphous precipitation products at 430 ºC (method *1.2*), two zirconium dioxide phases – t-ZrO_2 and m-ZrO_2 – are identified in all samples under study. The samples of this group have a similar crystallite size of ~13-15 nm. An exception is sample *1.2B*, prepared from zirconium butoxide, whose crystallites are significantly smaller in size (Table 1).

Table 1 – The phase composition of the zirconium dioxide samples prepared by different methods

Production method		Sample	Phase composition	Mole ratio, %	Crystallite size, nm
Precipitation in alcohol–ammonia medium	1.1	*1.1P*	-	-	-
		1.1B	-	-	-
		1.1Ch	-	-	-
		1.1N	-	-	-
Calcination of the Zr hydroxides obtained by method 1.1 at 430 ºC	1.2	*1.2P*	t-ZrO_2/m-ZrO_2	61/39	13,0
		1.2B	t-ZrO_2/m-ZrO_2	57/43	8,2
		1.2Ch	t-ZrO_2/m-ZrO_2	66/34	15,3
		1.2N	t-ZrO_2/m-ZrO_2	66/34	15,2
Ultrasound effect on the suspension of hydroxides Zr, hydrothermal ageing	2.1	*2.1P*	t-ZrO_2/m-ZrO_2	65/35	11,3
		2.1B	c-ZrO_2/m-ZrO_2	50/50	5,4
		2.1Ch	t-ZrO_2/m-ZrO_2	45/55	13,9
		2.1N	t-ZrO_2/m-ZrO_2	47/53	13,1
Use of ultrasound in the process of precipitation of Zr hydroxides in alcohol–ammonia medium, hydrothermal ageing	2.2	*2.2P*	m-ZrO_2	100	22,0
		2.2B	m-ZrO_2	100	38,4
		2.2Ch	m-ZrO_2	100	34,9
		2.2N	m-ZrO_2	100	35,1
Template hydrothermal synthesis in an alcohol-alkaline (alcohol–ammonia) medium at different ratios of components and hydrothermal ageing of the reaction mixture	3.1	*3.1P*	t-ZrO_2/m-ZrO_2	44/56	9,0
		3.1B	t-ZrO_2/m-ZrO_2	41/59	8,8
		3.1Ch	m-ZrO_2	100	9,3
		3.1N	t-ZrO_2/m-ZrO_2	62/38	13,9
	3.2	*3.2P*	t-ZrO_2/m-ZrO_2	22/78	28,9
		3.2B	t-ZrO_2/m-ZrO_2	39/61	22,3
		3.2Ch	t-ZrO_2/m-ZrO_2	40/60	13,7
		3.2N	t-ZrO_2/m-ZrO_2	52/48	13,0
	3.3	*3.3P*	t-ZrO_2/m-ZrO_2	40/60	6,6
		3.3 B	t-ZrO_2/m-ZrO_2	33/67	6,5
		3.3Ch	c-ZrO_2/m-ZrO_2	43/57	7,7
		3.3N	c-ZrO_2/m-ZrO_2	40/60	8,3

Figure 1 presents a typical zirconium dioxide X-ray diffraction pattern for samples *1.2P*, *1.2B* and *1.2N* of this group using *sample 1.2Ch* as an example. The X-ray diffraction pattern for samples *1.2P*, *1.2B* and *1.2N* look similar.

It is seen from Table 1 and Fig.1 that the ultrasound treatment of the aqueous suspension of the amorphous precipitation products and their subsequent hydrothermal ageing (method *2.1*) leads to the formation of zirconium dioxide crystalline phases at 250 ºC. In the case of Zr oxysalts, the nature of inorganic precursors does not practically matter. The crystal structure of the zirconium dioxide samples *2.1Ch* and *2.1N* synthesized in this way is represented by the tetragonal (t-ZrO_2) and monoclinic(m-ZrO_2) modifications in almost equal proportions, yet with some advantage of the latter.

When ZrO_2 is synthesized using zirconium propylate or butylate by method 2.1, the obtained samples exhibit some differences in their structure depending on the nature of alkoxides (Table 1, Fig.1). Apparently, the structural feature of samples *2.1P* and *2.1B* are determined in this case by the structure of the alkoxide groups. According to literature data [24], the number of metal atoms in a single polymer molecule in the solutions of initial n-propoxide and n-butoxide alcohols is equal to 2.44 and 1.77, respectively.

It was established in [25] that a mixture of two complexes (solvated dimer and trimer) is present in the Zr isopropoxide solutions. According to [26-28], the equilibrium in the Zr butoxide solution is shifted toward solvated dimer. The X-ray diffraction pattern of sample *2.1B*, synthesized using Zr butoxide, shows reflections that correspond to the cubic and monoclinic modifications of ZrO_2 in equal proportions.

Since the X-ray diffraction patterns of high-temperature zirconium oxide modifications c-ZrO_2 и t-ZrO_2 are very similar, the interpretation of the XRD results in favor of the cubic phase in sample *2.1B* is carried out based on the absence of bifurcation (characteristic of the tetragonal structure of ZrO_2) in reflections at $2\Theta=35^o$ and $2\Theta=60^o$. It is worth to note that sample *2.1B* has the smallest crystalline size (~5 nm) of all the materials examined. For sample *2.1P* prepared from zirconium propoxide, the X-ray diffraction method determines the tetragonal and monoclinic phases of ZrO_2, but the proportion of the high-temperature phase t-ZrO_2 is significantly higher than in samples *2.1N* and *2.1Ch*, where oxysalts were used as zirconium oxide precursors (Table 1, Fig.1).

The application of ultrasound directly to the process of precipitation of zirconium hydroxides (method 2.2) and subsequent hydrothermal ageing of the obtained precipitates at 250 ºC, regardless of the nature of precursors, lead to the formation of ZrO_2 in the monoclinic modification with largest, of all the samples considered in this work, crystallite size of 22-38 nm (Table 1). The X-ray patterns of the ZrO_2 samples prepared by this method are similar, as shown in Fig.1, where sample *2.2P* is used as an example.

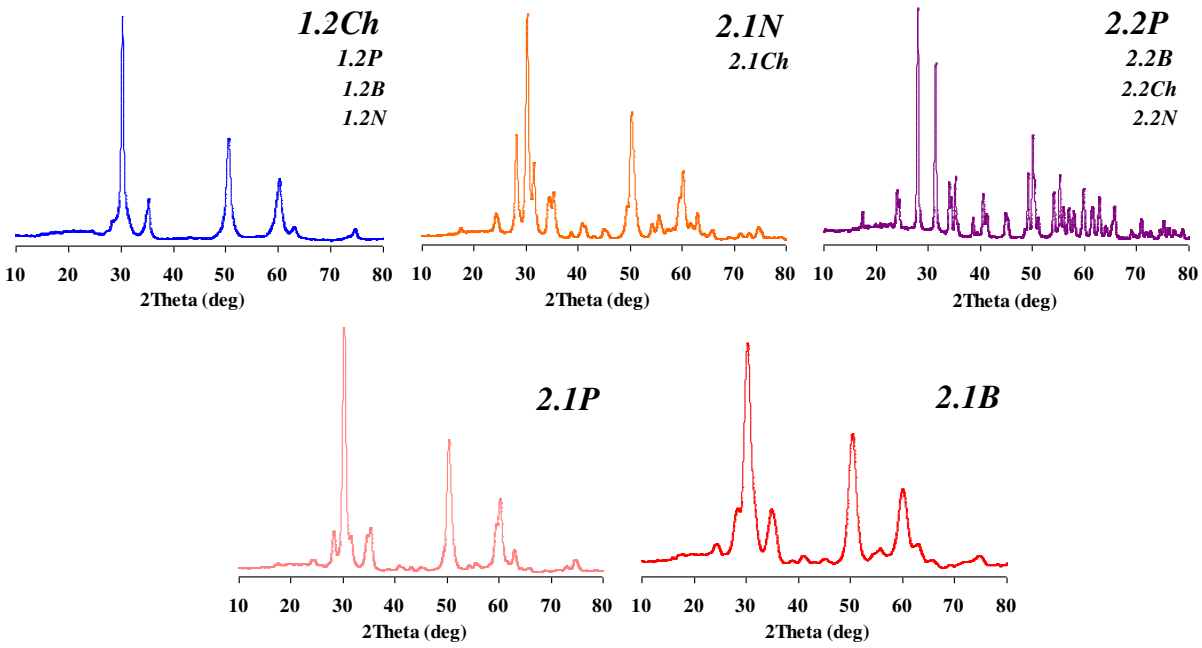

Fig. 1 - X-ray diffraction patterns of the ZrO_2 samples prepared by the template precipitation methods

The influence of the nature of Zr precursors and the effects of additional physical impact factors – ultrasound, hydrothermal ageing and calcinations – during the synthesis of zirconium dioxide samples by different template-free precipitation methods was evaluated when studying its textural and morphological properties (Tables 1, 2).

The nitrogen sorption-desorption isotherms of the samples *1.1P* and *1.1B*, prepared from zirconium alkoxides, as well as these samples but after calcination (*1.2P* и *1.2B),* can be assigned to type II (UPAC), which corresponds to the processes of free mono-polylayer adsorption. A long, close to horizontal, section on the adsorption-desorption isotherms and the curves of pore size distribution in these samples indicate the presence of micropores. A sharp rise in the curves in the range of relative pressures 0.9-1 characterizes the processes of nitrogen sorption-desorption in the interparticle space (Fig.2).

The sorption isotherms of the samples obtained by the same methods from zirconium oxysalts (samples *1.1N, 1.1Ch, 1.2N* and *1.2Ch*) can be assigned, according to UPAC, to type IV. Hysteresis on the sorption isotherms of these samples corresponds to type H2. The samples of this group are characterized by a narrow pore size distribution with a clearly defined maximum (Fig. 2B).

3.2 The textural properties of zirconium dioxide produced by through various methods of template-less precipitation synthesis

The textural properties of zirconium dioxide prepared by different variants of method 2 are mainly determined by a sequence of ultrasound effects during the process of zirconium oxide synthesis and are practically independent of the nature of precursors (Fig.2, Table 2).

Thus, the suspension of amorphous precipitation products is exposed to ultrasound (method 2.1), the shape of the sorption isotherms of the samples prepared from zirconium alkoxides (samples *2.1P* and *2.1B*), and from its oxysalts (samples *2.1Ch* and *2.1N*) can also be assigned to type IV (UPAC). The region of capillary condensation of nitrogen is shifted to the region of high relative pressures. Hysteresis on the sorption isotherms of the samples also corresponds to type H2 (UPAC) and indicates the presence of homogeneous mesopores with a narrow distribution of

their sizes. The average pore size in the zirconium alkoxide samples *2.1P* and *2.1B* is slightly less (4-6 nm) compared to the samples prepared from Zr oxysalts (~8 nm).

The isotherms of the samples *2.2P, 2.2B, 2.2Ch* and *2.2N* produced from zirconium alkoxides and from its oxysalts under ultrasound treatment directly in the process of precipitation (method 2.2) have the shape close to type III (UPAC), which is typical of non-porous and low-porous materials (Fig.2).

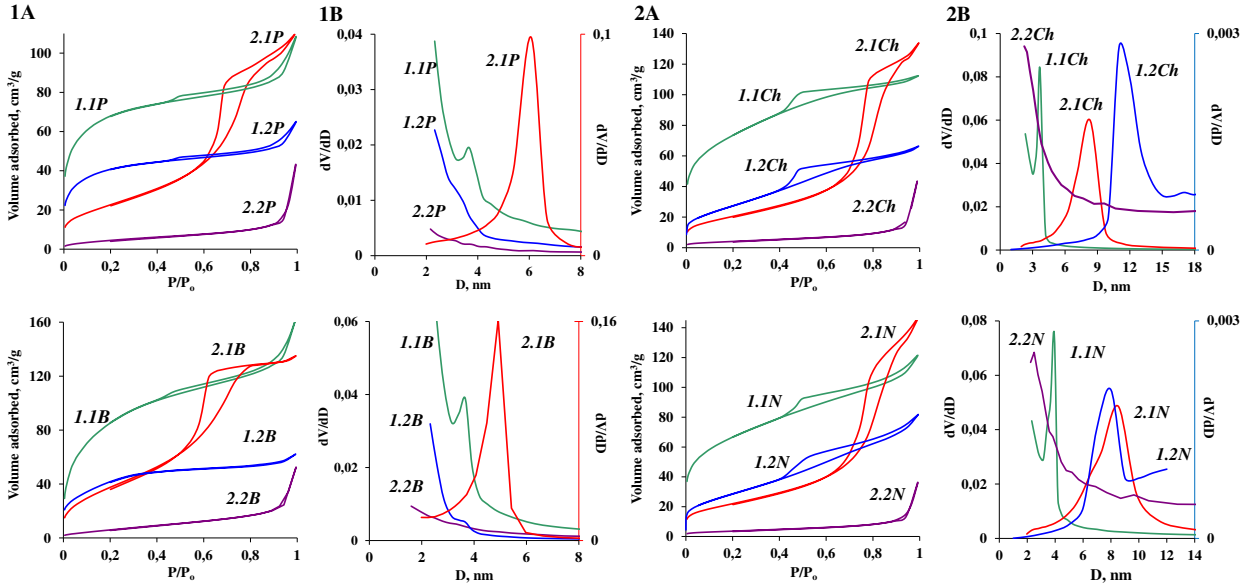

Fig.2 - Adsorption isotherms (1A, 2A) and pore size distribution (1B, 2B) for the ZrO_2, samples obtained from Zr alkoxides(A), Zr oxysalts (B) by different types of the templateless precipitation synthesis.

3.3 The textural and structural features of zirconium dioxide produced by through various methods of template methods

The results of a study of the textural and structural properties of the zirconium dioxide samples, which were fabricated in the water-base medium by different types of the template hydrothermal synthesis (method 3), demonstrate that these samples are significantly dependent on the ratio of the main components.

Figure 3 gives the X-ray diffraction patterns of the ZrO_2 samples prepared by method 3.1 at the mole ratio of the reaction medium components 100 H_2O : 0,44 CTAB : 0,4 NaOH : 1 Zr^{4+}, selected using the results of the synthesis of zirconium dioxide with a high specific surface [29].

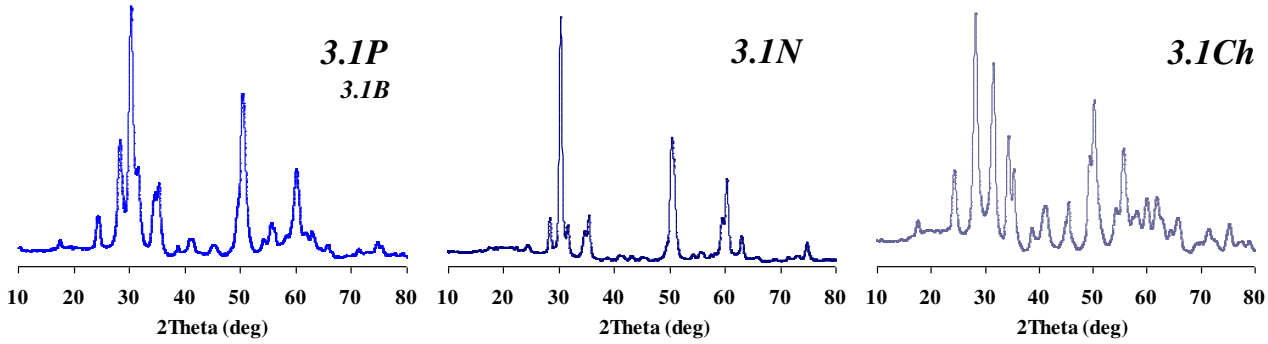

Fig. 3 - X-ray diffraction patterns of the ZrO_2 samples obtained by method 3.1

It is seen that two zirconium dioxide phases, t-ZrO_2 and m-ZrO_2, are identified in the samples *3.1P* and *3.1B* prepared using zirconium alkoxides, as well as in sample *3.1N*, where zirconyl nitrate dihydrate is used as a precursor. However, the proportion of a ZrO_2 tetragonal modification in sample *3.1N* is far greater. In the sample *3.1C* synthesized using zirconium oxychloride, only a ZrO_2 monoclinic modification with a small crystallite size is detected (Table 1).

At the same time, the sample *3.2Ch,* produced under alkaline hydrolysis in the presence of CTAB by applying hydrothermal ageing but with a greater number of NaOH cations, contains, in addition to the monoclinic modification of ZrO_2, its tetragonal modification (Fig.4).

The crystallite size in the samples *3.1P* and *3.1B*, obtained using zirconium alkoxides by method 3.1 under hydrothermal conditions is slightly smaller than in the samples *3.1N*, *3.1Ch,* fabricated by the same method but using Zr oxysalts. When a large amount of NaOH (method 3.2) is added to the reaction mixture, a reverse trend is being seen (Table 1).

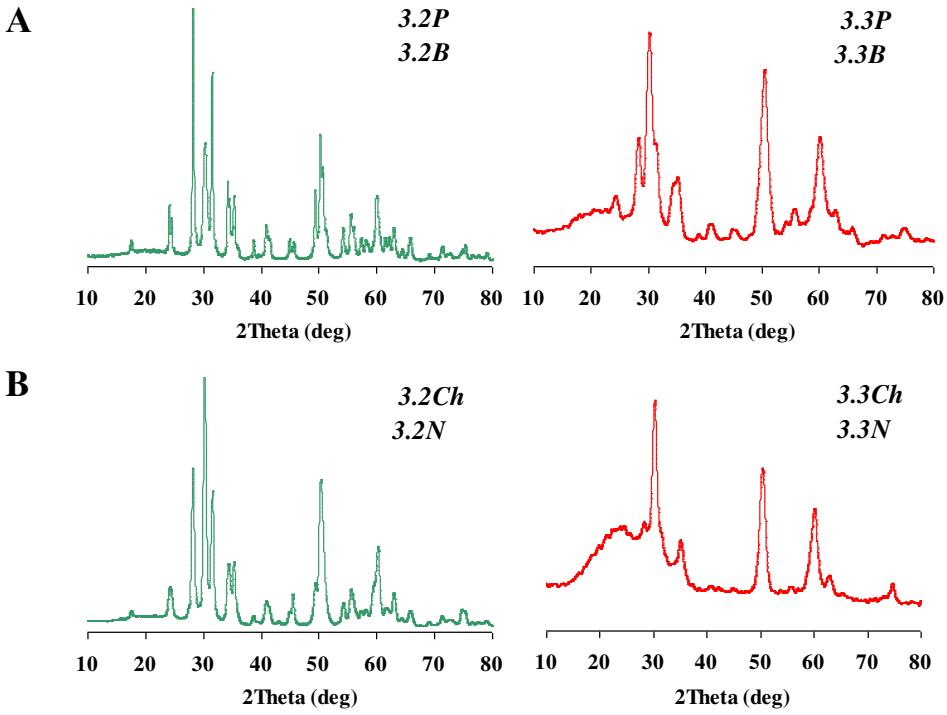

Fig. 4 - X-ray diffraction patterns of the ZrO_2 samples obtained by methods 3.2 and 3.3 using zirconium oxysalts (A) and zirconium oxysalts (B)

Of all the samples synthesized by different variants of method 3, the zirconium oxide samples prepared under hydrothermal conditions in the presence of CTAB but in a greater volume of an aqueous ammonia solution and, correspondingly, with a low concentration of precursors (method 3) have the smallest crystallite size (Table 1). In the ZrO_2 samples produced in this way, the X-ray diffraction method determines three phases of zirconium dioxide. In addition to the monoclinic and high-temperature phases of zirconium dioxide (t-ZrO_2, or c-ZrO_2) and despite the long-term high-temperature ageing (3 h, 650 ºC), the presence of amorphous compounds can be observed in the X-ray patterns as well. Furthermore, in the samples *3.3P* and *3.3B*, prepared from alkoxides Zr (Table 1, Fig. 4B), a tetragonal modification of ZrO_2 is determined, and in the samples *3.3Ch* and *3.3.N* made of oxysalts – cubic.

The textural and structural features of the zirconium dioxide samples prepared by different variants of method 3 in the presence of CTAB are most likely associated with the formation of different intermediate compounds that appear during the process of precipitation and subsequent hydrothermal ageing. The authors of

numerous papers, including [23, 30], support the view that the precipitation of hydroxides at pH>8 in the presence of surfactant cations is accompanied by the process of ion exchange due to electrostatic interactions. This promotes the formation of organic and non-organic compound, which, upon heating, loses water and an organic component and is converted into a non-organic oxide.

Figure 5 presents the IR-spectroscopy data for the zirconium dioxide samples, produced by different variants of method 3 and the IR-spectra of CTAB.

It is determined that the IR-spectra of CTAB are characterized by the absorption bands of 2872 cm^{-1} and 1432 cm^{-1}, which correspond to N-CH_3 bonds. The bands of 1486 cm^{-1} and 719 cm^{-1} correspond to the CH_2 groups of the carbon tail of surfactants. The bands in the 2850-3000 cm^{-1} region are assigned to methyl groups [30]. The vibration absorption bands corresponding to CTAB were present in all intermediate compounds during the synthesis of zirconium dioxide by different variants of method 3 and disappeared after calcination at 650 ºC (Fig.5, 6).

In the IR-spectra of all samples produced by different variants of method 3 and calcined 650 ºC, one can observe both the broad bands of 3432-3460 cm^{-1} and the bands of 1620-1637 cm^{-1} which correspond to the valence and deformation vibrations of water. According to existing literature, the bands in the 1430–1480 cm^{-1} region can be assigned to the deformation vibrations of the hydroxyl groups, which are related to the metal δ(ZrOH) involved in hydrogen bonding, and the bands in the 1300-1400 cm^{-1} region – to bridging OH-groups and hydroxide structured water [31].

The absorption bands in the frequency ranges 750-770 cm^{-1} and 580-680 cm^{-1} correspond to the valence ν(Zr–O) and deformation δ(O–Zr–O) vibrations, respectively, which indicates the formation of ZrO_2 [3, 32].

Figure 6 shows that the configurations of the IR spectra in the samples obtained from zirconium alkoxides by different variants of method 3 are similar. In the samples *3.2P* and *3.2B*, produced by the hydrothermal template method with an increased amount of a precipitation agent, one can observe a broad and intense band of ~1440 cm^{-1} that corresponds to the vibrations of hydroxide groups of the zirconium dioxide surface connected by hydrogen bonds. In the samples *3.1P* and *3.1B*, obtained with a smaller amount of the precipitant, the bands of 1458 (1461) cm^{-1} and 1345 (1350) cm^{-1}, corresponding to δ(ZrOH) and bridging hydroxides, are well identified.

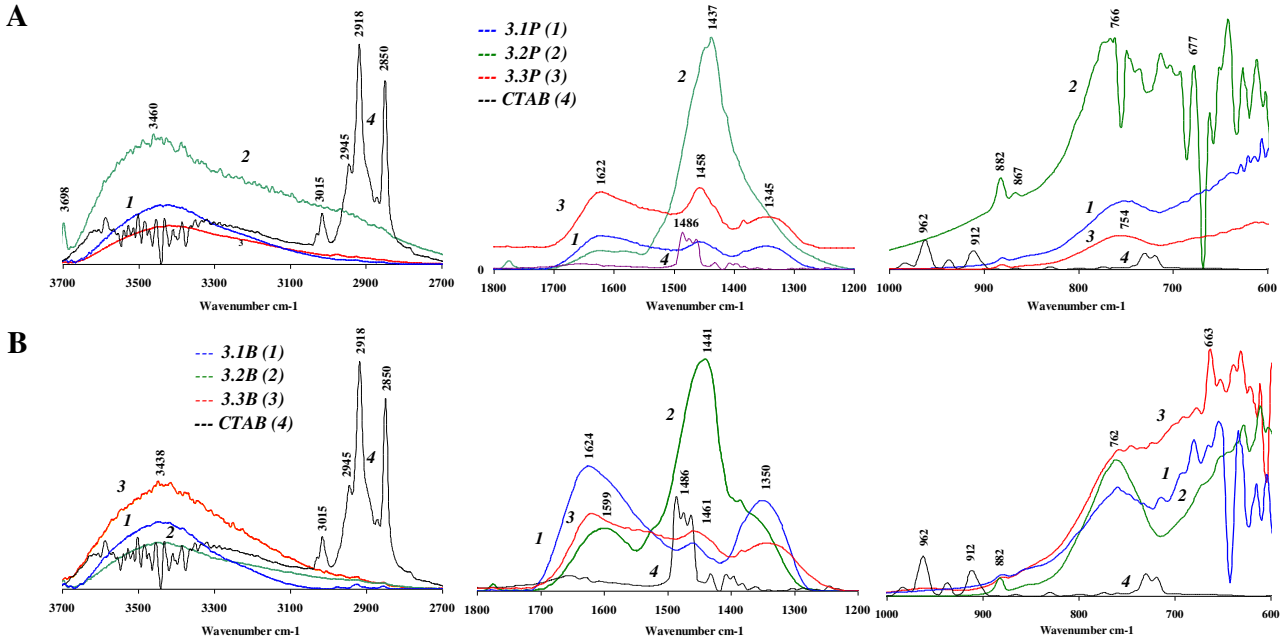

Fig. 5 – IR spectra of the zirconium dioxide samples obtained by different variants of the template hydrothermal synthesis using propylate (A), zirconium butylate (B)

The IR spectra of the calcined samples obtained by methods 3.1 and 3.2 from zirconium oxychloride octahydrate, regardless of the amount of a precipitant, are also identical (Fig.6A). A broad band of 812 cm^{-1} on the IR spectra of these samples is probably caused by the superposition of the absorption bands of deformation vibrations of Zr-OH and vibrations of Zr-O in groups Zr-O_2-Zr.

The IR spectra of samples *3.3Ch* и *3.3N* obtained by method 3.3 with a low concentration of zirconium oxysalts, regardless of the nature of the anion, are also identical (Fig.5, 6B).

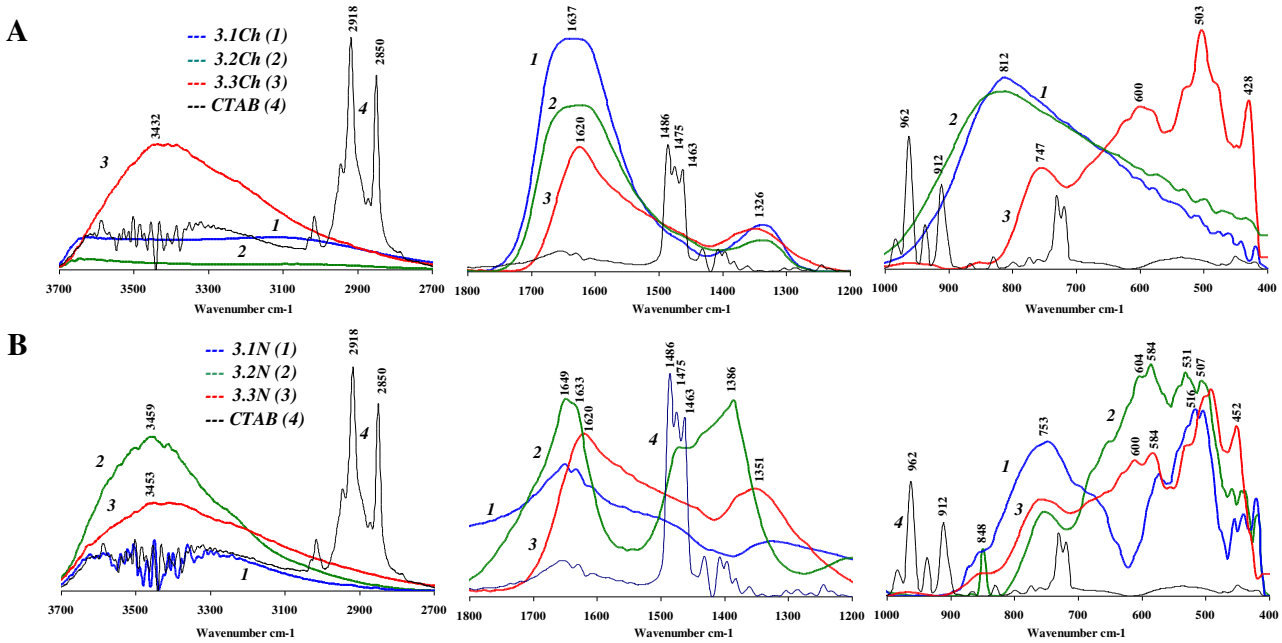

Fig. 6 – IR spectra of zirconium oxide samples prepared by different types of the template hydrothermal synthesis using zirconium oxychloride octahydrate (A) and zirconyl nitrate dehydrate (B)

The textural properties the zirconium dioxide samples produced by different variants of method 3 are shown in Fig.7 and summarized in Table 1. As one can see, the sorption-adsorption isotherms of the examined samples, except for sample *3.2N*, can be assigned to type IV (UPAC). Hysteresis on the sorption isotherms of the samples obtained by methods 3.1and 3.3., regardless of the nature of precursors, are more in line with type H2. This indicates that the porous structure is formed from tightly packing homogeneous primary particles that are close in size.

As depicted in Fig. 7A, the sorption isotherms and the pore size distribution curves for samples *1P* and *3.1B*, as well as for *3.2P* and *3.2B*, ZrO_2, prepared from zirconium alkoxides, practically coincide.

The textural properties of the zirconium dioxide samples *3.2Ch* and *3.2N* obtained by method 3.2 exhibit a certain dependence on the nature of the anion due to the probable interaction of the components of the reaction mixture under hydrothermal conditions and, consequently, on the structural features identified by IR spectroscopy (Fig.6).

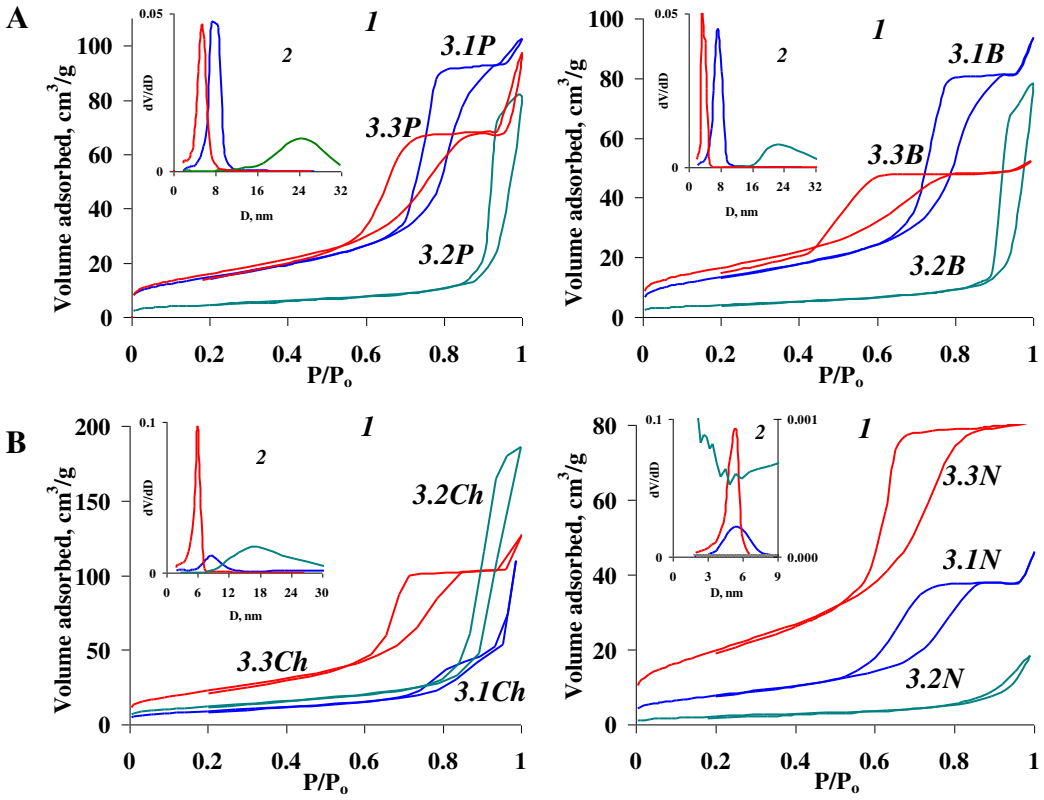

Fig. 7 – Sorption isotherms (1) and pore size distribution curves (2) for samples ZrO_2 prepared from alkoxides Zr (A) and oxysalts Zr (B) using different variants of method 3.

Table 2 – The textural properties of the zirconium dioxide samples prepared by different methods

Production method		Sample	Surface area, S_{BET}, m/g	Pore volume, V_{tot}, cm^3/g	Pore size, *D, nm*
Precipitation in the alcohol–ammonia medium	1.1	*1.1P*	203	0,29	9,3
		1.1B	280	0,26	5,0
		1.1Ch	236	0,17	3,5
		1.1N	214	0,19	4,4
Calcination of the Zr hydroxides obtained by method 1.1 at 430 ºC	1.2	*1.2P*	69	0,11	8,2
		1.2B	147	0,24	7,7
		1.2Ch	102	0,10	3,9
		1.2N	104	0,13	3,6
Ultrasound effect on the suspension of hydroxides Zr (*X, H*), hydrothermal ageing	2.1	*2.1P*	84	0,17	6,0
		2.1B	145	0,22	4,4
		2.1Ch	75	0,21	8,0
		2.1N	80	0,23	8,4
Use of ultrasound in the process of precipitation of Zr hydroxides in the alcohol–ammonia medium , hydrothermal ageing	2.2	*2.2P*	17	0,07	15,2
		2.2B	27	0,08	10,7
		2.2Ch	15	0,07	17,7
		2.2N	13	0,06	17
Template hydrothermal synthesis in the alcohol-	3.1	*3.1P*	*53*	0,16	7,4
		3.1B	*48*	0,14	7,1

alkaline (alcohol–ammonia) medium at different ratios of the components and subsequent hydrothermal ageing of the reaction mixture		*3.1Ch*	*32*	0,17	17
		3.1N	*28*	0,07	5,4
	3.2	*3.2P*	16	0,12	22
		3.2B	14	0,12	24
		3.2Ch	43	0,29	19,1
		3.2N	8	0,02	12,77
	3.3	*3.3P*	58	0,15	5,1
		3.3 B	59	0,08	4,0
		3.3Ch	83	0,2	5,4
		3.3N	72	0,13	4,9

The samples ZrO_2, which were obtained in the presence of CTAB by method 3.3 (Table 2, Fig.7), exhibit extra-large surface areas and narrow pore size distributions.

3.4 The morphological features of zirconium dioxide obtained by different methods

Figure 8 presents the SEM images of zirconium dioxide obtained by different template-free and template-based precipitation methods.

It is seen that, after deposition and drying at 100 ºC, the hydrated zirconium oxides – samples of group 1.1 (Fig.8A) – consist of particle aggregates of different sizes, which are larger in the case of zirconium alkoxides. After calcination of these samples at 430 ºC, the particle size is somewhat averaged (Fig.8B).

The particles of the samples obtained by method 2.1 (ultrasonic treatment of hydrated zirconium oxides produced by method 1.1 and subsequent hydrothermal ageing at 250 ºC) also have a round shape (particle size <100 nm) similar to samples *1.2P* and *1.2B*. All samples obtained by method 2.1 (ultrasound during the precipitation process and subsequent hydrothermal ageing) consist, regardless of the nature of precursors, of needle-shaped particles of the same size (Fig.8C).

The morphological features of ZrO_2 produced during the template hydrothermal synthesis by applying different variants of method 3 are similar, and they are shown in Fig.8D for the samples obtained by method 3.1. Samples *3.1P*, *3.1B*, where the ZrO_2 precursors are zirconium alkoxides, consist of equal-sized porous aggregates of round and spherical particles. The size of primary particles in these samples is ~ 40 nm, and the size of particle aggregates ranges from 0.8 to 1,5 μm. the size of the particle aggregates of a round shape in the samples *3.1Ch* and *3.1N*, prepared from zirconium oxisalts is somewhat less.

Fig. 8 – SEM images of the zirconium dioxide samples obtained by different methods

4. Conclusion

In this study, a comparative assessment of the textural-structural and morphological properties of the zirconium dioxide samples depending on the routes of its production and the nature of the precursors is given.

Methods of synthesizing zirconium dioxide with a small crystallite size (5-9 nm), a specific surface area ~ up to 150 m^2/g, and a pore volume up to 0.25 cm^3/g and with a narrow size distribution have been proposed.

It has been established that the nature of precursors observed in the case when zirconium dioxide is synthesized by different variants of the templateless precipitation method has a significant impact on its textural properties – the character of the sorption-desorption isotherms and the size pore distribution curves– and only slightly affect the phase composition of the samples. The phase composition of the samples mainly depends on the synthesis conditions of ZrO_2, including such additional physical factors as temperature, ultrasound, and hydrothermal ageing.

The use of ultrasound both at the precipitation stage and during the treatment of the suspension of pre-precipitated zirconium hydroxides leads to the formation of the crystalline structure of ZrO_2 at subsequent hydrothermal ageing stages at a temperature of ~ 250 ºC. In this case, the phase composition and morphology of the ZrO_2 sample particles depend on the priority of exposure to ultrasound. When ultrasound is applied directly during precipitation, the needle-shaped monoclinic ZrO_2 particles are formed. Under the action of ultrasound on a suspension of X-ray amorphous precipitation products (hydrated Zr oxides), the sample particles have a round shape. A phase composition in this case is represented by tetragonal and monoclinic modifications.

The nature of precursors of zirconium dioxide has a strong effect on its textural and structural properties in the case when the ZrO_2samples are prepared by applying different types of the template hydrothermal synthesis.

All ZrO_2 samples synthesized using different template hydrothermal treatment techniques are mesoporous. The method of producing zirconium dioxide from Zr alkoxides in the presence of a template (CTAB), followed by hydrothermal ageing, where 100 H_2O: 0.44 CTAB: 0.4 NaOH: 1 Zr^{4+}, holds promise for use in catalytic and sorption technologies. In this case, the zirconium dioxide samples consist of monodisperse particles ~ 40 nm in size, collected in equal-sized aggregates. The zirconium oxide samples produced by the template hydrothermal synthesis method using alkoxides and zirconium oxysalts with a low concentration of precursors in a large volume of ammonia solution have the smallest crystalline size (6-8 nm) and high specific surface (up to 83 m^2/g), but low yield in mass.

Funding

This research was financially supported by the State Contractual Order Nr. 124022200039-7.

Conflicts of interest/Competing interests

The authors have no conflict of interest to declare.

Availability of data and material

Not applicable

Code availability

Not applicable

Authors' contributions

Not applicable

Ethics approval

Not applicable

Consent to participate

Not applicable

Consent for publication

Not applicable

Author's information

Savastyanova Mariy, ORCID:https://orcid.org/0009-0007-9546-0964

Kondrashova Natalya, Candidate of chemical Sciences, ORCID:https://orcid.org/0000-0001-8535-8033

Ukhin Konstantin, Candidate of technical Sciences ORCID:https://orcid.org/0000-0001-8468-7513

Valtsifer Viktor, Doctor of technical Sciences, professor, ORCID:https://orcid.org/0000-0002-8671-739X

References

1. Liu J, Hensley AJR, Giannakakis G, Therrien AJ, Sukkar A, Schilling AC, Sykes ECH (2021) Developing single-site Pt catalysts for the preferential oxidation of CO: A surface science and first principles-guided approach. Appl Catal, B: Environmental 284:119716. https://doi.org/10.1016/j.apcatb.2020.119716
2. Bellmann A, Atia H, Bentrup U, Brückner A (2018) Mechanism of the selective reduction of NO_x by methane over Co-ZSM-5. Appl Catal, B: Environmental 230:184–193. https://doi.org/10.1016/j.apcatb.2018.02.051
3. Samson K, Śliwa M, Socha RP, Gora-Marek K, Mucha D, Rutkowska-Zbik D, Paul JF, Ruggiero-Mikołajczyk M, Grabowski R, Słoczynski J (2014) Influence of ZrO_2 Structure and Copper Electronic State on Activity of Cu/ZrO_2 Catalysts in Methanol Synthesis from CO_2. ACS Catal 4:3730−3741. https://doi.org/10.1021/cs500979c

4. Moretti E, Molina AI, Sponchia G, Talon A, Frattini R, Rodriguez-Castellon E, Storaro L (2017) Low-temperature carbon monoxide oxidation over zirconia-supported CuO–CeO_2 catalysts: Effect of zirconia support properties. Appl Surf Sci 403:612–622. https://doi.org/10.1016/j.apsusc.2017.01.095
5. Nezhad PDKh, Haghighi M, Rahmani F (2018) CO_2/O_2-Enhanced Ethane Dehydrogenation over Sol-Gel Synthesized Ni/ZrO_2- MgO Nanocatalyst: Effects of MgO, ZrO_2 and NiO on Catalytic Performance. Part Sci Technol 36:1017-1028. https://doi.org/10.1080/02726351.2017.1340376
6. Rahmani F, Haghighi M, Mohammadkhani B (2017) Enhanced dispersion of Cr nanoparticles over nanostructured ZrO_2-doped ZSM-5 used in CO_2-oxydehydrogenation of ethane. Microporous Mesoporous Mater 242:34–49. https://doi.org/10.1016/j.micromeso.2017.01.012
7. Toray H, Yoshimura M, Somiya S (1984) Calibration Curve for Quantitative Analysis of the Monoclinic–Tetragonal ZrO_2 System by X–Ray Diffraction. J Am Ceram Soc 67:119–121. https://doi.org/10.1111/j.1151-2916.1984.tb19715.x
8. Simonov YA, Kritsky AA, Rychkov VN, Tomashov VA, Chelpanov VV. Method of processing zircon to produce zirconium dioxide. Patent of the Russian Federation, 2434956
9. Khimich NN, Semashko OV, Khimich EN, Voronkov MG (2006) Sol-gel synthesis of dispersed ZrO_2 nanoparticles. Inorganic Synthesis and Industrial Inorganic Chemistry 79:351-355. https://doi.org/10.1134/S1070427206030025
10. Ivanov VK, Kopitsa GP, Baranchikov AE., Grigor'ev S.V., Haramus V.M. Evolution of Composition and Fractal Structure of Hydrous Zirconia Xerogels during Thermal Annealing // Russ. J. Inorg. Chem. 2010. V.55. № 2. P.155–161. https://doi.org/10.1134/S0036023610020038
11. Smit P.M., Zyl A., Kingon A.I. The hydrolysis of zirconium n–propoxide – Part 1. // Mater. Chem. Phys. 1987. V.17, Is.6., P.507–519. https://doi.org/10.1016/0254-0584(87)90010-1
12. Rubio F, Rubio J, Oteo JL (1998) Effect of reaction parameters on the hydrolysis of zirconium propoxide. A study by infrared spectroscopy. J Mater Sci Lett 17:1839–1842.
13. Gorokhova EV, Nazarov VV, Medvedkova NG, Kagramanov GG, Frolov YuG (1993) Synthesis and properties of zirconia hydrosol, obtained by hydrolysis of zirconium oxychloride. Colloid J 55:30–34.
14. Almjasheva OV, Fedorov BA, Smirnov AV, Gusarov VV (2010) Size, morphology and structure of the particles of zirconia nanopowder obtained under hydrothermal conditions. Nanosystems: Physics, Chemistry, Mathematics. 1:26–36.
15. Bagchi B, Basu RN (2015) A simple sol–gel approach to synthesize nanocrystalline 8 mol% yttria stabilized zirconia from metal–chelate precursors: Microstructural evolution and conductivity studies. J Alloys Compd 647:620–626. https://doi.org/10.1016/j.jallcom.2015.06.082
16. Fabrichnaya O, Kriegel MJ, Pavlychkov D, Seidel J, Djuban A, Savinykh G, Schreiber G (2013) Heat capacity for the $Eu_2Zr_2O_7$ and phase relations in the ZrO_2 – Eu_2O_3 system: Experimental studies and calculations. Thermochim Acta 558:74-82. https://doi.org/10.1016/j.tca.2013.02.009
17. Mondal A, Zachariah P, Nayak BB, Nayak J (2010) Synthesis and Room Temperature Photoluminescence of Mesoporous Zirconia with a Tetragonal Nanocrystalline Framework. J Am Ceram Soc 93:387–392. https://doi.org/10.1111/j.1551-2916.2009.03396.x
18. Guel ML, Jiménez LD, Hernández DAC (2017) Ultrasound–assisted sol–gel synthesis of ZrO_2. Ultrason Sonochem 35A:514–517. https://doi.org/10.1016/j.ultsonch.2016.09.010

19. Baranchikov AY, Kopitsa GP, Ivanov VK (2018) Ultrasonic treatment as method of structure change of amorphous materials prepared by sol-gel. Chemical Engineering 19(13):608-614. https://doi.org/10.31044/1684-5811-2018-19-13-608-614
20. Gubanova NN, Baranchikov AY, Kopitsa GP, Almásy L, Angelov B, Yapryntsev AD, Rosta L, Ivanov VK (2015) Combined SANS and SAXS study of the action of ultrasound on the structure of amorphous zirconia gels. Ultrason Sonochem 24:230–237. https://doi.org/10.1016/j.ultsonch.2014.11.012
21. Aghabeygi S, Khademi–Shamami M (2018) ZnO/ZrO_2 nanocomposite: Sonosynthesis, characterization and its application for wastewater treatment. Ultrason Sonochem 41:458–465. https://doi.org/10.1016/j.ultsonch.2017.09.020
22. Shabanova NA, Popov VV, Sarkisov PD (2006) Chemistry and technology of nanodisperse oxides. ICTS Akademkniga, Moscow.
23. Turova NYa, Turevskaya EP, Kessler VG, Yanovskaya MI (2002) Hydrolysis of Metal Alkoxides and Synthesis of Simple Oxides by The Sol– Gel Method in book The Chemistry of Metal Alkoxides. The Chemistry of Metal Alkoxides:107–125. https://doi.org/10.1007/0-306-47657-6_9
24. Bradley DC, Mehrotra RC, Wardlaw W (1952) Structural chemistry of the alkoxides. Part I. Amyloxides of silicon, titanium, and zirconium. J Chem Soc:2027–2032. https://doi.org/10.1039/JR9520002027
25. Peter D, Ertel TS, Bertagnolli H (1994) EXAFS study of zirconium alkoxides as precursor in the sol-gel process: I. Structure investigation of the pure alkoxides. J of Sol-Gel Sci and Technology 3:91-99. https://doi.org/10.1007/BF00486715
26. Peter D, Ertel TS, Bertagnolli H (1995) EXAFS study of zirconium alkoxides as precursors in the sol-gel process: II. The influence of the chemical modification. Journal of Sol-Gel Science and Technology 5(1):5-14. https://doi.org/10.1007/BF00486706
27. Reinöhl U, Ertel TS, Hörner W, Weber A, Bertagnolli H (1998) EXAFS investigation of mixed zirconium-titanium alkoxides. Ber Bunsenges Phys Chem 102:144-147. https://doi.org/10.1002/bbpc.19981020203
28. Rose J, De Bruin TJM, Chauveteau G (2003) Aqueous Zirconium Complexes for Gelling Polymers. A Combined X-ray Absorption Spectroscopy and Quantum Mechanical Study. J Phys Chem B 107:2910-2920. https://doi.org/10.1021/jp027114c
29. Kondrashova N, Saenko E, Lebedeva I, Valtsifer V, Strelnikov V (2012) Effect of organic-silane additives on textural-structural properties of mesoporous silicate materials. Microporous and mesoporous materials 153:275-281. https://doi.org/10.1016/j.micromeso.2011.12.017
30. Borjas-García SE, Medina-Flores A, Béjar L, Martínez-Torres P, Dasgupta-Schubert N, Bernal JL, Bruce W, O´hare D, Walton RI (2010) Synthesis of Mesoporous Ceria by Using CTAB as Template. Microsc Microanal 359:2016. https://doi.org/10.1017/S1431927616010436
31. Krut'ko VK, Kulak AI, Musskaya ON (2017) Thermal transformations of composites based on hydroxyapatite and zirconia. Inorganic Materials 53:427–434 https://doi.org/10.7868/S0002337X17040091
32. Venina dos Santos, Bergmann CP (2012) Synthesis and Characterization of Crystalline Zirconium Titanate Obtained by Sol-Gel. Advances in Crystallization Prcesses: 301–314. https://doi.org/10.5772/36385